1995AJ....109..543B

THE ASTRONOMICAL JOURNAL VOLUME 109, NUMBER 2 FEBRUARY 1995

TOTAL AND EFFECTIVE COLORS OF 501 GALAXIES IN THE COUSINS *VRI* PHOTOMETRIC SYSTEM

R. BUTA

University of Alabama, Tuscaloosa, Alabama 35487-0324
Electronic mail: buta@sarah.astr.ua.edu

KESHA L. WILLIAMS

Jackson State University, Jackson, Mississippi 39217-0460

Received 1994 September 9; revised 1994 October 25

ABSTRACT

Total color indices $(V-R)_T$, $(V-I)_T$ and effective color indices $(V-R)_e$, $(V-I)_e$ in the Cousins *VRI* photometric system are presented for 501 mostly normal galaxies. The colors are computed using a procedure outlined in the Third Reference Catalogue of Bright Galaxies (RC3) whereby standard color curves approximated by Laplace–Gauss integrals are fitted to observed photoelectric multiaperture photometry. 11 sources of such photometry were used for our analysis, each source being assigned an appropriate weight according to a rigorous analysis of residuals of the data from the best-fitting standard color curves. Together with the integrated $B-V$ and $U-B$ colors provided in RC3, our analysis widens the range of wavelength of homogeneously defined colors of normal galaxies of all Hubble types. We present color–color and color–type relations that can be modeled to understand the star formation history of galaxies.

1. INTRODUCTION

The star formation history of galaxies is contained in the integrated color of their present-day composite stellar populations. It is now believed that the correlation between the corrected total color indices $(B-V)_T^\circ$ and $(U-B)_T^\circ$ in the conventional two-color diagram reflects in large measure the locus of galaxies of similar age having monotonically decreasing star formation rates [Searle *et al.* 1973; Larson & Tinsley 1978; Kennicutt 1983; see also Aaronson (1978) and Charlot & Bruzual (1991) for a discussion of the $U-V$, $V-K$ two-color plot]. A large body of homogeneous data in the *UBV* photometric system now exists to more accurately establish the correlation (see Buta *et al.* 1994a). However, a lesser, but still significant body of integrated photometry also exists in the Cousins *VRI* photometric system (see Bessell 1979) that has not yet been fully tapped for the interpretation of the star formation history of galaxies. Models of the color evolution of galaxies could be better constrained if a wider baseline of *homogeneously defined* integrated colors of normal galaxies was available.

In this paper, we use the Cousins *VRI* photometry compiled by de Vaucouleurs & Longo (1988), supplemented by more recent data, to derive well defined total and effective $V-R$ and $V-I$ color indices that are directly comparable to the $U-B$ and $B-V$ color indices presented in the Third Reference Catalogue of Bright Galaxies (de Vaucouleurs *et al.* 1991, hereafter referred to as RC3). Buta *et al.* (1995) have described the methods by which the total and effective $U-B$ and $B-V$ colors were computed for ≈3000 galaxies using a large database of published and unpublished multiaperture photoelectric photometry. The basic procedure involved extrapolating the total (or asymptotic) colors by fitting to such data mean curves which approximate the color gradients typically found (de Vaucouleurs & Corwin 1977). From these curves the effective colors, defined as the colors within a circular aperture, A_e, which transmits half the total blue luminosity, can usually be interpolated. It turns out that the same procedures can be used to derive total and effective $V-R$ and $V-I$ colors. A preliminary discussion of the application of RC3 methods to the redder passband colors for a small sample of outer-ringed galaxies is given by Buta & Crocker (1992).

2. METHODOLOGY

Photoelectric Cousins *VRI* multiaperture photometry involves the use of a standard photoelectric photometer [e.g., RCA 31034A plus filters listed by Bessell (1979), or equivalent systems] to measure the apparent fluxes of galaxies in circular diaphragms of different sizes. If the size of an aperture is comparable to the angular size of a galaxy, then the colors will closely approximate the total colors. If the size of an aperture is equal to the effective aperture diameter, A_e, then the effective colors will be equal to the colors measured in that aperture. However, as noted by de Vaucouleurs & Corwin (1977), it is often impractical to use an aperture that is as large or larger than the isophotal diameter of a galaxy, and without prior knowledge of A_e, one cannot choose an appropriate aperture for the effective colors. Thus, the only way to get total and effective colors is to fit mean curves which provide an estimate of how integrated colors behave on average over the widest possible range of apertures, from $A<A_e$ to $A>D_0$, the standard "face-on" isophotal diameter (de Vaucouleurs *et al.* 1976, hereafter referred to as RC2).

The standard integral color curves used in RC2 and RC3 (see Fig. 4 of de Vaucouleurs & Corwin 1977) were derived from about 3000 *UBV* photoelectric observations of nearly

 0004-6256/95/109(2)/543/15/$0.90 © 1995 Am. Astron. Soc.

© American Astronomical Society • Provided by the NASA Astrophysics Data System

1995AJ....109..543B

TABLE 1. Sources of *VRI* photometry.

Source Code	Reference	n($V-R$)	n($V-I$)
BCR–92	Buta and Crocker 1992	145	145
BUT–84[a]	Buta, unpublished Siding Spring Observatory observations	16	16
COR–84[a]	Corwin, unpublished McDonald Observatory observations	342	342
COR–93	Corwin, unpublished McDonald Observatory observations	126	126
GRD–78	Green and Dixon 1978	74	74
LAU–84	Lauberts 1984	769	680
MMM–83	McAlary et al. 1983	24	23
POU–86	Poulain 1986	658	640
POU–88	Poulain 1988	882	875
RSM–82[a]	Smyth 1982, unpublished Siding Spring Observatory observations	230	221
SCK–91	Schroder and Kepler 1991	57	56

Notes to TABLE 1

[a] Measurements provided in de Vaucouleurs and Longo (1988)

500 galaxies. The galaxies were divided by Hubble type T, and all aperture diameters were normalized to A_e. It was found that the curves could be well approximated by Laplace–Gauss integrals with different total amplitudes depending on type. The curves were first derived for $U-V$, and then apportioned between $B-V$ and $U-B$. The value of A_e must be known before applying these curves to observed multiaperture data. Thus, there is an important preliminary step involved before deriving total and effective colors. A_e is derived by fitting mean standard "growth curves" to B-band photoelectric photometry. Magnitude growth curves provide information on how the integral of the flux of a galaxy changes or grows as the size of the measuring aperture is increased. Like the color curves, they also depend on Hubble type [see Fig. 1(a) of de Vaucouleurs (1977) and Fig. 5(a) of RC2, and for updated curves see Fig. 2 and Table 11 of the Introduction to RC3]. Since the integral flux can increase rapidly with increasing aperture, the derivation of A_e depends critically on the range of apertures which are available to define the growth curve of a particular galaxy. If this photometry has too few small apertures or too few large apertures, then A_e will be uncertain. However, even significant uncertainties in A_e do not translate to large uncertainties in total and effective colors because integrated color gradients in galaxies tend to be small.

With the publication of RC3, A_e is available for nearly 2600 galaxies. About 500 of these have integrated $V-R$ and $V-I$ multiaperture photometry available that could be used to derive total and effective colors. An important question is, what standard color curves do we use for such photometry? In principal, we could derive the appropriate curves using the same procedure described by de Vaucouleurs & Corwin (1977) for $B-V$ and $U-B$ colors. However, the $V-R$, $V-I$ sample is heavily weighted towards early Hubble types such that some later types have little data on which to base the analysis. We instead explored applying to $V-R$ and $V-I$ the same curves that were used for $B-V$ and $U-B$. It turns out that because the typical color gradients in $V-R$ and $V-I$ are bracketted by those in $B-V$ and $U-B$, this is an entirely feasible procedure. Buta & Crocker (1992) illustrated this for 36 ringed galaxies by using standard $B-V$ curves for $V-R$ fits and standard $U-B$ curves for $V-I$ fits. We decided, then, to use the same procedure for all available $V-R$ and $V-I$ photometry, with one improvement over Buta & Crocker (1992): we added zero integrated color gradient curves to each set of $B-V$ and $U-B$ curves to allow for this possibility in the $V-R$ and $V-I$ photometry. This gave 17 total curves in each color over all types.

3. SOURCES OF PHOTOMETRY

Table 1 lists the sources of photometry we have used for our analysis. The main database was extracted from the catalogue of de Vaucouleurs & Longo (1988). This compilation includes sources available only through the end of 1985. Major sources of Cousins *VRI* photometry that have been published since 1985 (up to mid 1993, the time when we carried out this work) include Poulain (1986, 1988), Schroder & Kepler (1991), and Buta & Crocker (1992).[1] In addition, Corwin (1993) sent to us his complete list of unpublished *UBVRI* photometry, a major portion of which was included in the de Vaucouleurs and Longo catalogue under the source COR-84. From all sources, we had 3200 $V-R$ and 3075 $V-I$ measurements to work with.

4. DERIVATION OF SOURCE WEIGHTS AND WEIGHTING FUNCTIONS

The different sources of photometry in Table 1 involved different photometers, telescopes, observational procedures, aperture sizes, and, most importantly, different types of galaxies that will affect the uncertainties of the measurements. For example, sources LAU-84, POU-86, and POU-88 include mainly early-type galaxies of high average surface brightness, while sources COR-84 and RSM-82 include mostly late-type spirals of low average surface brightness. In addition, the former sources tended to observe their samples

[1] An extensive set of *BVI* data obtained by Visvanathan (1992) for 178 galaxies towards the so-called "Great Attractor" has not been used in our analysis owing to a lack of $\log A_e$ information and a generally limited coverage in $\log A$ for each galaxy.

© American Astronomical Society • Provided by the NASA Astrophysics Data System

1995AJ....109..543B

TABLE 2. Galaxies with non-RC3 $\log A_e$'s.

Galaxy	B_T	$\log A_e$	Notes
IC 1091	14.51	0.62	1
IC 2035	12.48	0.27	1
IC 5011=IC 5013	12.84	0.49	2
IC 5065	14.58	0.29	3
IC 5161	11.44V[a]	0.68	1
IC 5269	13.17	0.81	1
NGC 274	12.08:V[a]	0.79	1
NGC 1179	12.63	1.24	3
NGC 1380B	12.49:V[a]	1.14	1
NGC 2673	14.1::	0.71:	1
NGC 2924	13.08	0.98	1
NGC 3171	13.8::	0.93:	4
NGC 3300	13.44	0.72	1
NGC 3630	13.07	0.49	1
NGC 3957	12.84	0.85	1
NGC 4441	13.37	0.87	3
NGC 5757	12.79	0.74	1
NGC 6854	13.2::	0.97:	4
NGC 6876	11.5::	1.36:	1
NGC 7225	13.0::	0.97:	4
NGC 7339	13.13	0.89	3
NGC 7393	13.48	0.73	1
NGC 7633	13.67:	0.60	4
ESO 479– 33	14.55	0.25	3
ESO 484– 7	16.64	0.19	3

Notes to TABLE 2

1. Parameters newly determined
2. Parameters omitted from RC3 because of identity mismatch
3. $\log A_e$ omitted from RC3 because of extrapolation
4. Parameters omitted from RC3 because of excessive extrapolation to B_T

[a] V-band total magnitude

with relatively small apertures ($A<1'.5$) while COR-84 and RSM-82 used apertures up to 4′ in angular diameter. Photometry with large apertures tends to have lower signal-to-noise ratio than photometry with small apertures because large apertures include a greater proportion of sky noise and possible contaminating field objects than small apertures. Thus, any fits of standard color curves to observed photometry must be weighted according to the observer, the telescope used, the brightness of the galaxy in a given aperture, and the average surface brightness of the galaxy in a given aperture.

The total and effective $B-V$ and $U-B$ colors in RC3 were computed using weights derived from error functions taking into account the above effects. The equations that were used are summarized by Buta *et al.* (1995) (see also Sec. 3.7 of the Introduction to RC3). We have derived similar equations for the $V-R$ and $V-I$ colors. The procedure was as follows. First, we extracted all available values of $\log A_e$ for our sample galaxies from machine version RC3.9a. Although source POU-88 provided full *UBVRI* photometry for a significant sample of galaxies that was not used in the computation of RC3 parameters (owing to the cutoff date of 1987), we have not recomputed values of B_T and $\log A_e$ for these galaxies because many were well observed previously and the apertures used by Poulain were not large. It was also our desire to provide $V-R$ and $V-I$ colors that were homogeneous with the parameters already listed in RC3. For a few galaxies where $\log A_e$ is not available in RC3, we fitted the B magnitudes with standard growth curves and derived B_T and $\log A_e$. These objects are summarized in Table 2 under Note 1. Table 2 lists a few other objects which had $\log A_e$ information that was not entered in the final version of RC3, usually because excessive extrapolation was involved. We have used the approximate $\log A_e$ values for these galaxies (derived by RB during the course of RC3 production) because the errors in $\log A_e$ will not translate to large errors in the integrated $V-R$ and $V-I$ parameters.

In the second step, we combined the new sources of photometry with the information already contained in the de Vaucouleurs and Longo catalogue and created separate files of those galaxies having four or more available measurements and those having three or less measurements. Any galaxy with four or more measurements was considered well observed and suitable for the error analysis and weight derivation. The standard color curves were then fitted to the observed $V-R$ and $V-I$ colors for the well observed galaxies using the same program that was used for the computation of total and effective $B-V$ and $U-B$ colors in RC3. The program adopts the curve which best fits the data, and writes out the total and effective colors as well as the residuals of the observed data about the curves. The fits were made in three iterations. In the first iteration, all measurements were assigned unit weight regardless of source, magnitude, telescope, or surface brightness. A large file of residuals from these unit weight fits was saved, and plots were made of them for quick checking. For most of the well observed galaxies, the range of $\log A$ available was sufficient to define the color gradients well. Measurements having $\log A/A_e<-0.5$ were not included in the fits.

Following RC3, we chose sources with a sufficient range in magnitude, surface brightness, and number of observations to define the error functions for $V-R$ and $V-I$. The best sources for this purpose were Poulain, Lauberts, and Corwin, who provided complementary samples in the sense that most of Poulain's and Lauberts' photometry involves mean surface brightnesses brighter than 13 mag arcmin^{-2}, while most of Corwin's photometry involves mean surface brightnesses fainter than 12 mag arcmin^{-2}. Figures 1 and 2 illustrate the absolute value of the $V-R$ and $V-I$ residuals, respectively, about the fits vs V-band magnitude and mean V-band surface brightness (mag arcmin^{-2}) defined as

$$m'(V)=V+5\ \log A-5.26. \tag{1}$$

The dependence of the average deviation on magnitude and especially mean surface brightness is obvious in these plots. As in the analysis of $B-V$ and $U-B$ colors, we chose hyperbolic functions to represent these dependences, as follows.[2] If we let $\alpha=|O-C|$, the residuals, then the following functions were adopted to represent the average deviations:

$$\alpha(V-R)=a_0+a_1(f_V-\langle f_V\rangle)+a_2(f_{m'}-\langle f_{m'}\rangle), \tag{2a}$$

$$\alpha(V-I)=b_0+b_1(f_V-\langle f_V\rangle)+b_2(f_{m'}-\langle f_{m'}\rangle), \tag{2b}$$

where

[2]In Buta *et al.* (1995), the error functions were based on fits involving the calculated magnitude, $B_c(A)$, derived from the best-fitting standard growth curve to the B-magnitude data, rather than the observed $B(A)$ magnitude. Here we use the observed $V(A)$ magnitude because all of the sources of the *VRI* photometry are modern and because no separate fits were made to the V magnitudes alone.

© American Astronomical Society • Provided by the NASA Astrophysics Data System

1995AJ....109..543B

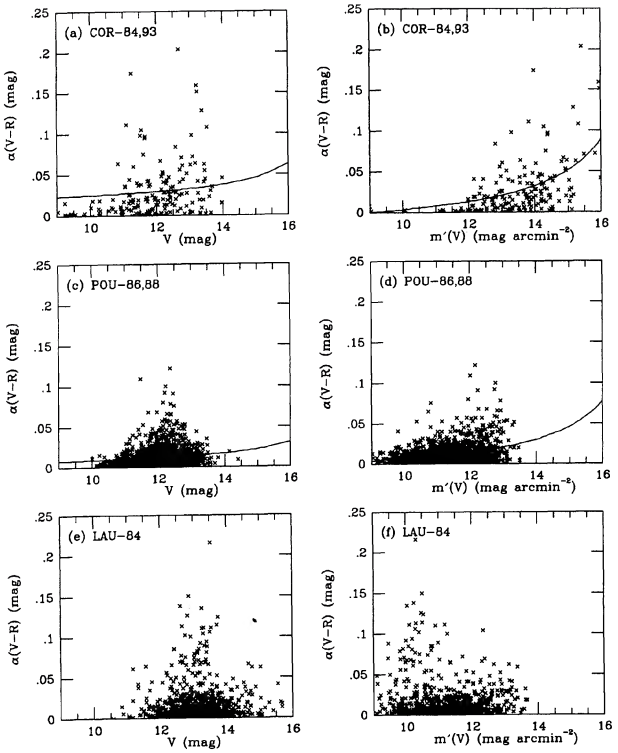

FIG. 1. Absolute value of residuals of $V-R$ colors about best-fitting standard curves, plotted vs apparent V magnitude and mean V-band surface brightness. Curves are based on least squares fits of Eq. 2(a) to the data. Since these are two-dimensional fits, the curves in (a), (c), and (e) are based on the $\langle f_{m'} \rangle$ values for each sample, while the curves in (b), (d), and (e) are based on the $\langle f_V \rangle$ values for each sample.

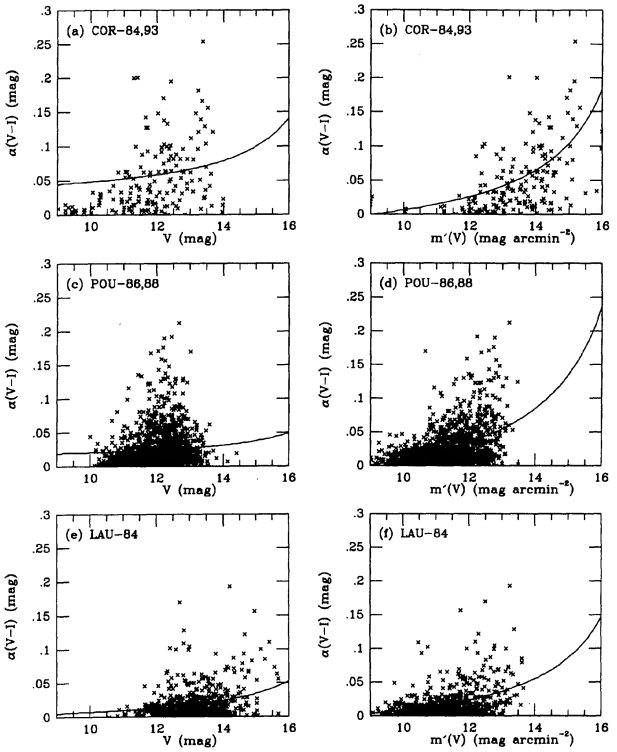

FIG. 2. Absolute value of residuals of $V-I$ colors about best-fitting standard curves plotted vs apparent V magnitude and mean V-band surface brightness. Curves are based on least squares fits of Eq. 2(b) to the data. Since these are two-dimensional fits, the curves in (a), (c), and (e) are based on the $\langle f_{m'} \rangle$ values for each sample, while the curves in (b), (d), and (e) are based on the $\langle f_V \rangle$ values for each sample.

$$f_V = \frac{1}{c_1 + 5\ \log(D/0.76) - V}, \tag{2c}$$

$$f_{m'} = \frac{1}{c_2 - m'(V)}. \tag{2d}$$

In Eq. (2c), D is the diameter of the telescope objective mirror. It is normalized to the McDonald Observatory 0.76 m telescope which was used for Corwin's observations. The asymptote constants c_1 and c_2 were chosen to coincide roughly with a magnitude about 1 mag fainter than the limiting visual magnitude of a 0.76 m telescope and a limiting surface brightness of about 0.5% of the night sky brightness. We chose $c_1 = 18.0$ mag and $c_2 = 18.0$ mag arcmin^{-2}.

The constants a_1, a_2, b_1, and b_2 were derived by fitting Eqs. (2a) and (2b) to the residuals plotted in Figs. 1 and 2. Allowing for the differences in the telescope apertures used, the three sources of photometry illustrated gave the values listed in Table 3 (see also the curves plotted in Figs. 1 and 2). For $V-I$, the sources were fairly consistent, but for $V-R$, the photometry of Lauberts contains some large errors that prevent Eq. (2a) from being used. Thus, we have averaged the values from all three sources for $V-I$, but for $V-R$ have averaged only the coefficients from the Poulain and Corwin photometry. The results show that the errors in the $V-R$ photometry are much less sensitive to magnitude and surface brightness than those in $V-I$ photometry.

With the mean coefficients in Table 3, we can now reduce the average deviations for all sources in Table 1 to the same levels of magnitude and mean surface brightness, and thereby compute a pure source-dependent weight. Using $V = 12.0$ mag and $m'(V) = 12.0$ mag arcmin^{-2} as representative of the whole database of the observations, we computed for each source values of the following parameters:

$$\alpha_0(V-R) = \alpha(V-R) - 0.08(f_V - 0.17) - 0.19(f_{m'} - 0.17), \tag{3a}$$

$$\alpha_0(V-I) = \alpha(V-I) - 0.15(f_V - 0.17) - 0.52(f_{m'} - 0.17). \tag{3b}$$

TABLE 3. Coefficients of Equations 2(a) and 2(b).

Coefficient	COR	LAU	POU	weighted means
a_1	0.102 ±0.100	–	0.082 ±0.021	0.083 ±0.021
a_2	0.231 ±0.042	–	0.189 ±0.016	0.194 ±0.015
b_1	0.246 ±0.197	0.169 ±0.036	0.106 ±0.046	0.147 ±0.028
b_2	0.472 ±0.083	0.369 ±0.049	0.608 ±0.036	0.519 ±0.027

© American Astronomical Society • Provided by the NASA Astrophysics Data System

1995AJ....109..543B

TABLE 4. Reduced average deviations and source weights.

Source	$\alpha_o(V-R)$	n$(V-R)$	$w_o(V-R)$	$\alpha_o(V-I)$	n$(V-I)$	$w_o(V-I)$	D(m)
BCR-92	0.008	20	2.0	0.014	20	2.0	1.00
BUT-84	0.004	10	2.0	0.045	10	0.3	0.60
COR-84,93	0.017	177	1.0	0.025	177	1.0	0.76
GRD-78	0.016	57	1.1	0.046	57	0.3	1.00
LAU-84	0.020	696	0.7	0.025	618	1.0	1.00
MMM-83	0.014	13	1.5	0.066	13	0.1	0.75
POU-86,88	0.017	1451	1.0	0.037	1431	0.5	1.00
RSM-82	0.023	74	0.5	0.048	68	0.3	0.40
SCK-91	0.024	47	0.5	0.046	46	0.3	1.60

Table 4 lists the resulting values of the reduced average deviations, and the numbers of residuals involved in their computation. We define unit weight observations by Corwin's data, and thus set $\alpha_{01}(V-R)=0.017$ mag and $\alpha_{01}(V-1)=0.025$ mag. Then for each source and color index, the reduced weight was computed as

$$w_0=(\alpha_{01}/\alpha_0)^2. \quad (4)$$

Values of w_0 are listed in Table 4. To avoid excessive weights for some sources with rather few observations compared to others, we set the maximum reduced weight allowed to 2.0. The actual weight for a given observation i by source j was derived from Eq. (26) of the Introduction to RC3:

$$w_{ij}=w_{0j}(1+f_i\sqrt{w_{0j}}/\alpha_{01})^{-2}, \quad (5)$$

where

$$f_i(V-R)=0.08(f_V-0.17)+0.19(f_{m'}-0.17), \quad (6a)$$

$$f_i(V-I)=0.15(f_V-0.17)+0.52(f_{m'}-0.17). \quad (6b)$$

Following RC3, we allowed a maximum weight of 4.0 for the observations from the best sources of the brightest galaxies having the highest surface brightness.

With known reduced weights and weighting functions, we then refit all observations and computed a new file of residuals. In this second approximation, we attempted to determine whether any of the sources required significant zero point corrections. For this purpose, we used only those galaxies in the well observed sample which had two or more sources of photometry. We were unable to use the restriction to four or more sources that was adopted in RC3 because very few galaxies in our $V-R$, $V-I$ sample had more than two sources of photometry. The results showed that only the photometry of Green & Dixon (1978, hereafter referred to as GRD-78) required significant corrections: +0.012 mag for $V-R$ and −0.006 mag for $V-I$. These corrections are subtracted from the published GRD-78 photometry, and were included in the third and final iteration. We also fitted in the final iteration all galaxies with three or two observations, and used the results only if the available apertures covered enough of a range to define a color gradient. Plots were made for every case and were inspected carefully. In a few cases where the number of small apertures greatly exceeded the number of large apertures, we increased the minimum allowed value of $\log A/A_e$ for the fits to better balance the points. In cases where no color measurements were in apertures larger than A_e, we rejected the total colors because of excessive required extrapolation. For the same reason, we also rejected effective colors if all of the available apertures greatly exceeded A_e in diameter.

5. COMPILATION OF PARAMETERS

Table 5 (Table 5 is presented in its complete form in the AAS CD-ROM Series, Volume 4, 1995) lists the final derived parameters for 501 galaxies. Internal mean errors (m.e.) of the total colors were derived as $const./\sqrt{\Sigma w}$, where Σw is the sum of the weights of all measurements having $\log A/A_e \geq 0$, and $const=0.02$ and 0.03 for $V-R$ and $V-I$, respectively. Internal errors for the effective colors were similarly derived, but using Σw for the range $-0.5 \leq \log A/A_e \leq 0.5$. Because in most cases the effective colors were derived by interpolation, we expect them to have better *external* precision than total colors. However, the external errors cannot be computed because we have few independent estimates of these colors, for example from surface photometry, that could be used to derive these errors. We expect the external errors in the total colors to be of order ±0.05 mag in some cases, depending on galaxy type, the size of the color gradient, and the amount of extrapolation.

Columns 12 and 13 in Table 5 provide information on the standard color curves (SCC) which best fit the data for each galaxy. Column 12 gives the type index for the $B-V$ curve used to fit the $V-R$ data while Column 13 gives the type index for the $U-B$ curve used to fit the $V-I$ data. In both columns, $T(\text{SCC})=20$ refers to the zero color gradient fits, and the index is only meant to distinguish these from the original de Vaucouleurs and Corwin set of color curves. The serious disagreement between these "colorimetric types" and the catalogue types in column 2 should not be considered alarming because the curves were not originally defined by $V-R$ and $V-I$ photometry. Nevertheless, the number of early type galaxies that were best fit by the inverse color gradient curves of Magellanic spirals and irregulars (types 9 and 10, respectively) is noteworthy. Since the color gradients are typically small in early-type galaxies, some inverse gradients will be expected from even small observational errors.

© American Astronomical Society • Provided by the NASA Astrophysics Data System

1995AJ....109..543B

TABLE 5. Total and effective $V-R$ and $V-I$ color indices for 501 galaxies.*

Object	RC3 Type	N	$(V-R)_T$	m.e.	$(V-I)_T$	m.e.	$(V-R)_e$	m.e.	$(V-I)_e$	m.e.	T(SCC) $B-V$	T(SCC) $U-B$
1	2	3	4	5	6	7	8	9	10	11	12	13
NGC 59	−3	6	0.44	0.012	0.85	0.016	0.40	0.012	0.82	0.016	10	10
NGC 80	−3	5	0.53	0.009	1.34	0.019	0.60	0.009	1.34	0.019	5	20
NGC 83	−5	5	0.65	0.010	1.44	0.022	0.65	0.010	1.42	0.022	20	9
NGC 100	6	5	0.50	0.032	0.96	0.067	–	–	–	–	20	20
NGC 125	−1	3	–	–	–	–	0.54	0.011	1.17	0.022	9	10
NGC 128	−2	8	0.56	0.005	1.15	0.010	0.57	0.005	1.24	0.010	−4	3
NGC 134	4	2	0.56	0.026	1.27	0.055	–	–	–	–	20	20
NGC 147	−5	3	–	–	–	–	0.55	0.016	1.12	0.032	20	10
NGC 148	−2	18	0.56	0.004	1.16	0.006	0.54	0.004	1.18	0.006	9	7
NGC 185	−5	2	–	–	–	–	0.60	0.018	1.23	0.029	20	10
NGC 210	3	3	0.44	0.019	1.02	0.039	0.53	0.019	1.09	0.039	4	5
NGC 216	−2	5	0.43	0.012	0.83	0.016	0.38	0.012	0.83	0.016	10	20
NGC 227	−3	4	0.52	0.010	1.24	0.019	0.58	0.010	1.24	0.019	2	20
NGC 235	−2	3	0.55	0.013	1.11	0.014	0.56	0.013	1.19	0.014	−5	2
NGC 254	−1	15	0.56	0.004	1.15	0.005	0.54	0.004	1.15	0.005	9	20
NGC 274	−3	9	0.48	0.006	1.11	0.012	0.56	0.006	1.20	0.012	4	3
NGC 289	4	2	0.47	0.028	1.05	0.067	–	–	–	–	3	3
NGC 323	−5	4	0.61	0.011	1.31	0.010	0.61	0.011	1.29	0.010	20	10
NGC 324	0	12	0.47	0.033	1.17	0.011	0.42	0.033	1.21	0.011	10	−3
NGC 337A	8	2	0.30	0.045	0.78	0.095	0.38	0.063	0.88	–	4	3
NGC 439	−3	9	–	–	–	–	0.58	0.009	1.24	0.010	8	8
NGC 474	−2	7	0.55	0.008	1.22	0.020	0.55	0.008	1.20	0.021	20	10
NGC 484	−3	4	0.59	0.009	1.24	0.008	0.59	0.009	1.24	0.008	20	20
NGC 488	3	3	0.52	0.014	1.13	0.024	0.60	0.014	1.23	0.024	4	3
NGC 524	−1	5	–	–	–	–	0.62	0.005	1.36	0.009	7	7
NGC 533	−5	5	–	–	–	–	0.51	0.009	1.17	0.019	4	3
NGC 568	−3	4	–	–	–	–	0.57	0.015	1.24	0.019	20	10
NGC 584	−5	12	0.57	0.003	1.19	0.005	0.57	0.003	1.20	0.005	20	8
NGC 596	−4	14	0.58	0.003	1.24	0.005	0.56	0.003	1.21	0.005	9	10
NGC 613	4	3	0.52	0.018	1.03	0.036	0.55	0.018	1.12	0.036	1	3
NGC 625	9	2	0.41	0.032	0.84	0.067	–	–	–	–	10	10
NGC 636	−5	9	0.56	0.005	1.24	0.008	0.56	0.005	1.22	0.008	20	10
NGC 641	−3	7	0.53	0.009	–	–	0.49	0.009	–	–	10	–
NGC 678	3	4	0.70	0.019	1.39	0.039	–	–	–	–	−5	20
NGC 691	4	2	0.43	0.026	1.04	0.055	0.51	0.037	1.07	0.067	4	7
NGC 697	5	3	0.57	0.020	1.20	0.039	0.66	0.026	1.29	0.047	4	3
NGC 720	−5	17	0.57	0.003	1.18	0.006	0.58	0.003	1.23	0.006	−5	6
NGC 741	−5	4	–	–	–	–	0.64	0.011	1.34	0.023	9	8
NGC 772	3	4	0.56	0.012	1.14	0.019	0.59	0.012	1.20	0.019	0	5
NGC 821	−5	5	–	–	–	–	0.61	0.007	1.25	0.012	−3	4
NGC 936	−1	7	0.58	0.005	1.22	0.008	0.58	0.005	1.23	0.008	20	8
NGC 988	6	4	0.38	0.015	0.82	0.027	–	–	–	–	20	20
NGC 1023	−3	2	0.58	0.011	1.22	0.014	–	–	–	–	6	3
NGC 1024	2	3	0.72	0.022	1.39	0.042	0.67	0.028	1.37	0.047	10	10
NGC 1031	1	4	0.51	0.010	1.15	0.029	0.58	0.010	1.22	0.029	3	5
NGC 1052	−5	13	0.56	0.003	1.22	0.005	0.59	0.003	1.26	0.005	0	−3
NGC 1055	3	3	0.62	0.018	1.28	0.036	0.60	0.018	1.25	0.036	9	10
NGC 1079	0	9	0.54	0.005	1.14	0.010	0.56	0.005	1.18	0.010	−2	6
NGC 1097	3	5	0.50	0.009	1.07	0.018	0.56	0.009	1.17	0.018	2	3
NGC 1156	10	4	0.46	0.015	0.92	0.025	0.46	0.015	0.92	0.026	20	20
NGC 1172	−4	8	0.51	0.007	1.20	0.015	0.55	0.007	1.23	0.015	1	7
NGC 1179	6	4	0.41	0.028	1.01	0.067	0.41	0.028	1.01	0.067	20	20
NGC 1199	−5	4	0.66	0.008	1.33	0.015	0.62	0.008	1.30	0.015	10	10
NGC 1201	−2	9	0.56	0.004	1.20	0.006	0.57	0.004	1.22	0.006	−4	8
NGC 1209	−5	4	0.57	0.007	1.27	0.013	0.59	0.007	1.25	0.013	−5	10
NGC 1232	5	2	0.41	0.024	0.94	0.055	0.49	0.032	1.03	0.067	4	3
NGC 1249	6	2	0.31	0.037	0.63	0.095	–	–	–	–	4	6
NGC 1256	−3	4	0.60	0.013	1.19	0.015	0.56	0.013	1.23	0.015	10	−4
NGC 1265	−4	8	0.67	0.015	1.37	0.025	0.69	0.015	1.46	0.025	−2	4
NGC 1291	0	2	0.53	0.015	1.16	0.027	0.58	0.020	1.21	0.034	6	1
NGC 1316	−2	10	–	–	–	–	0.58	0.019	1.17	0.032	4	3
NGC 1317	1	9	0.51	0.004	1.19	0.007	0.58	0.004	1.22	0.007	5	7
NGC 1326	−1	9	0.54	0.004	1.13	0.006	0.56	0.004	1.16	0.006	−3	7
NGC 1332	−3	21	0.58	0.004	1.28	0.005	0.61	0.004	1.28	0.005	0	20
NGC 1337	6	4	0.45	0.026	1.03	0.055	0.43	0.026	–	–	9	20
NGC 1339	−4	4	0.53	0.007	1.22	0.014	0.56	0.007	1.20	0.014	1	10
NGC 1344	−5	15	0.53	0.003	1.14	0.004	0.54	0.003	1.15	0.004	−4	8
NGC 1351	−3	14	0.54	0.004	1.12	0.006	0.55	0.004	1.17	0.006	−5	−5
NGC 1366	−2	8	0.56	0.005	1.19	0.005	0.54	0.005	1.17	0.005	9	10
NGC 1374	−5	9	0.58	0.004	1.15	0.007	0.56	0.004	1.20	0.007	9	−4
NGC 1375	−2	9	0.50	0.007	1.03	0.014	0.50	0.007	1.07	0.014	20	−4
NGC 1379	−5	13	–	–	–	–	0.57	0.004	1.19	0.007	10	10
NGC 1380	−2	21	0.55	0.003	1.18	0.004	0.57	0.003	1.21	0.004	8	7

© American Astronomical Society • Provided by the NASA Astrophysics Data System

1995AJ....109..543B

TABLE 5. (continued)

Object	RC3 Type	N	$(V-R)_T$	m.e.	$(V-I)_T$	m.e.	$(V-R)_e$	m.e.	$(V-I)_e$	m.e.	T(SCC) $B-V$	T(SCC) $U-B$
1	2	3	4	5	6	7	8	9	10	11	12	13
NGC 1380B	0	4	–	–	–	–	0.56	0.013	1.18	0.027	10	10
NGC 1381	−2	4	0.55	0.006	1.20	0.011	0.56	0.007	1.20	0.012	−3	20
NGC 1386	−1	4	0.53	0.007	1.19	0.012	0.57	0.007	1.19	0.012	1	20
NGC 1387	−3	14	0.60	0.003	1.26	0.005	0.62	0.003	1.31	0.005	−2	1
NGC 1389	−3	11	0.53	0.004	1.16	0.006	0.54	0.004	1.16	0.006	−5	20
NGC 1395	−5	4	–	–	–	–	0.58	0.005	1.24	0.008	−5	8
NGC 1399	−5	13	0.57	0.003	1.23	0.005	0.58	0.003	1.25	0.005	−5	8
NGC 1400	−3	4	0.63	0.006	1.38	0.011	0.63	0.006	1.36	0.011	20	10
NGC 1404	−5	4	0.57	0.005	1.23	0.008	0.57	0.005	1.23	0.008	20	20
NGC 1411	−3	21	0.56	0.003	1.15	0.006	0.51	0.003	1.14	0.006	10	9
NGC 1415	0	5	0.58	0.008	1.26	0.017	0.61	0.008	1.29	0.017	1	7
NGC 1426	−5	4	0.53	0.007	1.11	0.014	0.54	0.007	1.16	0.014	−2	0
NGC 1427	−4	9	0.53	0.005	1.11	0.006	0.54	0.005	1.15	0.006	−5	−4
NGC 1439	−5	4	0.51	0.008	1.13	0.016	0.54	0.008	1.16	0.016	0	7
NGC 1453	−5	4	0.63	0.008	1.41	0.015	0.65	0.008	1.39	0.015	−2	10
NGC 1461	−2	4	0.61	0.008	1.17	0.015	0.61	0.008	1.27	0.015	20	3
NGC 1515	4	3	0.56	0.024	1.27	0.055	–	–	–	–	7	10
NGC 1521	−5	4	0.52	0.009	1.21	0.018	0.58	0.009	1.19	0.018	2	10
NGC 1527	−3	5	0.57	0.005	1.22	0.008	0.57	0.005	1.22	0.008	20	20
NGC 1533	−3	19	0.57	0.003	1.19	0.005	0.58	0.003	1.22	0.005	−5	7
NGC 1537	−3	14	0.54	0.003	1.12	0.005	0.55	0.003	1.16	0.005	−5	−2
NGC 1543	−2	14	0.57	0.003	1.21	0.007	0.57	0.003	1.21	0.007	20	20
NGC 1546	−1	9	–	–	–	–	0.61	0.007	1.25	0.015	1	3
NGC 1549	−5	22	0.53	0.002	1.14	0.004	0.55	0.002	1.17	0.004	−3	7
NGC 1553	−2	13	0.52	0.004	1.05	0.008	0.54	0.004	1.13	0.008	−1	2
NGC 1560	7	6	0.50	0.016	0.98	0.034	0.50	0.016	1.03	0.034	20	1
NGC 1571	−4	5	0.54	0.009	1.13	0.008	0.56	0.009	1.21	0.008	0	2
NGC 1574	−3	9	0.56	0.003	1.23	0.006	0.57	0.003	1.22	0.006	−5	9
NGC 1587	−5	10	0.61	0.005	1.29	0.009	0.62	0.005	1.29	0.009	−4	20
NGC 1595	−5	6	0.58	0.010	1.20	0.011	0.56	0.011	1.20	0.011	9	20
NGC 1596	−2	9	0.56	0.004	1.18	0.006	0.57	0.004	1.21	0.006	−4	7
NGC 1600	−5	14	–	–	–	–	0.61	0.004	1.27	0.008	20	9
NGC 1638	−2	9	0.53	0.007	1.10	0.013	0.54	0.007	1.15	0.013	−4	6
NGC 1672	3	4	0.40	0.015	0.90	0.030	0.48	0.015	0.99	0.030	4	3
NGC 1700	−5	9	0.56	0.004	1.23	0.007	0.58	0.004	1.21	0.007	−1	10
NGC 1705	−3	7	0.26	0.008	0.59	0.007	0.22	0.008	0.56	0.007	10	10
NGC 1726	−2	14	0.61	0.004	1.27	0.008	0.61	0.004	1.27	0.008	20	20
NGC 1808	1	5	0.55	0.007	1.14	0.019	0.63	0.007	1.27	0.012	4	3
NGC 1930	−2	4	0.56	0.010	1.17	0.009	0.57	0.010	1.21	0.009	−2	−4
NGC 1954	4	3	0.60	0.021	1.26	0.042	0.57	0.021	1.35	0.042	9	3
NGC 1964	3	3	0.45	0.024	0.99	0.047	–	–	–	–	20	20
NGC 2090	5	4	0.56	0.018	1.14	0.039	–	–	–	–	10	10
NGC 2146A	5	2	0.42	0.032	0.78	0.067	0.38	0.037	0.87	0.067	10	3
NGC 2217	−1	15	0.60	0.003	1.23	0.005	0.61	0.003	1.28	0.005	−2	1
NGC 2310	−2	16	0.57	0.004	1.22	0.006	0.57	0.004	1.22	0.006	20	20
NGC 2325	−5	10	–	–	–	–	0.63	0.007	1.34	0.014	−5	20
NGC 2336	4	1	–	–	–	–	0.54	0.032	1.12	0.067	4	4
NGC 2377	5	4	0.65	0.016	1.24	0.029	0.68	0.017	1.33	0.030	0	3
NGC 2403	6	3	–	–	–	–	0.44	0.015	0.98	0.018	4	3
NGC 2434	−5	10	0.67	0.004	1.39	0.008	0.67	0.004	1.42	0.008	20	7
NGC 2442	4	4	0.57	0.019	1.24	0.042	0.63	0.019	1.34	0.042	6	3
NGC 2502	−2	5	0.78	0.008	1.64	0.008	0.78	0.008	1.65	0.008	20	8
NGC 2541	6	2	0.38	0.026	0.78	0.047	0.39	0.032	0.87	0.067	−2	3
NGC 2608	3	5	0.44	0.014	0.92	0.025	0.52	0.014	1.01	0.025	4	3
NGC 2613	3	3	0.56	0.021	1.25	0.042	0.64	0.021	1.34	0.042	4	3
NGC 2655	0	3	0.56	0.009	1.15	0.012	0.57	0.009	1.16	0.012	−5	8
NGC 2672	−5	8	0.62	0.005	1.27	0.010	0.62	0.005	1.27	0.010	20	20
NGC 2673	−5	3	–	–	–	–	0.56	0.013	1.22	0.026	5	3
NGC 2715	5	4	0.52	0.016	1.00	0.030	0.50	0.016	1.08	0.030	9	2
NGC 2717	−3	4	0.64	0.009	1.40	0.009	0.64	0.009	1.39	0.009	20	9
NGC 2749	−5	10	0.50	0.006	1.09	0.012	0.56	0.006	1.18	0.012	6	3
NGC 2768	−5	2	–	–	–	–	0.58	0.019	1.22	0.030	10	10
NGC 2781	−1	15	0.56	0.003	1.19	0.006	0.57	0.003	1.20	0.006	−2	8
NGC 2784	−2	13	0.67	0.003	1.43	0.005	0.69	0.003	1.45	0.005	−5	8
NGC 2805	7	2	–	–	–	–	0.41	0.045	0.90	0.095	4	10
NGC 2835	5	3	0.39	0.024	0.94	0.047	0.45	0.024	0.92	0.047	2	10
NGC 2842	0	4	0.58	0.010	1.24	0.009	0.62	0.010	1.29	0.009	1	1
NGC 2859	−1	3	0.56	0.013	1.11	0.018	0.57	0.016	1.18	0.021	−4	2
NGC 2865	−5	5	0.57	0.006	1.15	0.010	0.53	0.006	1.13	0.010	10	10
NGC 2891	−3	4	0.50	0.009	1.11	0.009	0.50	0.009	1.11	0.009	20	20
NGC 2902	−2	10	0.56	0.006	1.20	0.011	0.60	0.006	1.26	0.011	7	5
NGC 2904	−3	4	0.61	0.011	1.34	0.010	0.62	0.011	1.35	0.010	−4	8
NGC 2911	−2	14	0.58	0.008	1.19	0.047	0.64	0.008	1.28	0.047	5	3

© American Astronomical Society • Provided by the NASA Astrophysics Data System

1995AJ....109..543B

TABLE 5. (continued)

Object	RC3 Type	N	$(V-R)_T$	m.e.	$(V-I)_T$	m.e.	$(V-R)_e$	m.e.	$(V-I)_e$	m.e.	T(SCC) $B-V$	T(SCC) $U-B$
1	2	3	4	5	6	7	8	9	10	11	12	13
NGC 2924	−4	10	0.51	0.006	1.12	0.013	0.56	0.006	1.21	0.013	6	3
NGC 2962	−1	5	0.64	0.008	1.25	0.016	0.62	0.008	1.30	0.016	9	0
NGC 2974	−5	10	0.67	0.003	1.27	0.006	0.62	0.003	1.28	0.006	10	8
NGC 2976	5	2	0.52	0.015	1.05	0.026	0.52	0.020	1.02	0.032	20	10
NGC 2983	−1	9	0.59	0.004	1.23	0.007	0.59	0.004	1.25	0.007	20	8
NGC 2986	−5	5	0.60	0.006	1.26	0.011	0.60	0.006	1.27	0.011	20	8
NGC 3003	4	3	0.35	0.021	0.89	0.042	0.41	0.021	0.86	0.042	6	10
NGC 3027	7	3	0.36	0.024	0.73	0.055	0.36	0.024	0.80	0.055	20	2
NGC 3044	5	3	0.42	0.024	1.03	0.047	0.50	0.024	1.00	0.047	4	10
NGC 3056	−1	5	0.52	0.006	1.21	0.011	0.56	0.006	1.20	0.011	7	9
NGC 3067	2	2	0.51	0.021	1.14	0.039	–	–	–	–	4	10
NGC 3078	−5	5	0.59	0.005	1.32	0.009	0.61	0.005	1.31	0.009	−2	9
NGC 3079	7	3	0.53	0.013	1.14	0.022	0.60	0.013	1.24	0.022	5	3
NGC 3081	0	10	0.54	0.005	1.15	0.008	0.56	0.005	1.19	0.008	−1	−3
NGC 3087	−4	7	0.54	0.006	1.20	0.006	0.60	0.006	1.26	0.006	5	5
NGC 3091	−5	5	0.60	0.006	1.27	0.011	0.60	0.006	1.27	0.011	20	20
NGC 3115	−3	23	0.58	0.002	1.22	0.004	0.60	0.003	1.25	0.004	−3	7
NGC 3136	−5	5	0.66	0.006	1.32	0.010	0.64	0.006	1.34	0.010	9	7
NGC 3156	−2	5	0.47	0.008	1.00	0.017	0.45	0.008	0.99	0.017	9	9
NGC 3166	0	3	0.56	0.015	1.20	0.025	–	–	–	–	4	10
NGC 3171	−3	4	–	–	–	–	0.62	0.017	1.31	0.023	9	10
NGC 3184	6	3	0.40	0.017	0.90	0.030	0.48	0.017	1.00	0.030	4	3
NGC 3198	5	3	0.44	0.014	0.92	0.024	0.50	0.014	1.01	0.024	2	3
NGC 3200	5	4	0.51	0.020	1.10	0.042	0.59	0.028	1.19	0.055	4	3
NGC 3203	−1	5	0.58	0.008	1.26	0.014	0.59	0.008	1.25	0.014	−5	9
NGC 3227	1	2	0.50	0.018	1.06	0.034	0.58	0.024	1.15	0.042	4	3
NGC 3250	−5	5	0.58	0.005	1.30	0.009	0.62	0.005	1.34	0.009	7	−4
NGC 3254	4	3	0.48	0.019	1.03	0.036	0.56	0.019	1.12	0.036	4	3
NGC 3258	−5	5	0.61	0.007	1.29	0.015	0.62	0.007	1.32	0.015	−5	7
NGC 3268	−5	6	0.53	0.013	1.16	0.029	0.61	0.014	1.26	0.030	4	3
NGC 3271	−2	5	0.62	0.006	1.29	0.012	0.63	0.006	1.32	0.012	−5	7
NGC 3300	−2	5	0.47	0.009	1.12	0.019	0.55	0.009	1.21	0.019	4	3
NGC 3305	−5	3	0.64	0.022	–	–	–	–	–	–	10	–
NGC 3308	−3	3	0.65	0.018	–	–	0.63	0.018	–	–	9	3
NGC 3309	−5	7	0.49	0.007	1.17	0.014	0.57	0.007	1.26	0.014	4	3
NGC 3311	−4	2	–	–	–	–	0.64	0.032	–	–	9	–
NGC 3319	6	3	–	–	–	–	0.38	0.045	0.81	0.095	7	7
NGC 3338	5	3	0.44	0.022	0.96	0.042	0.52	0.022	1.05	0.042	4	3
NGC 3344	4	3	0.40	0.011	0.94	0.017	0.47	0.011	1.04	0.017	5	3
NGC 3359	5	3	0.37	0.015	0.85	0.026	0.41	0.015	0.87	0.026	1	8
NGC 3365	6	4	0.48	0.028	0.92	0.067	0.49	0.028	0.92	0.067	−4	20
NGC 3377	−5	5	0.52	0.005	1.10	0.007	0.54	0.005	1.14	0.007	−3	6
NGC 3379	−5	5	0.60	0.004	1.23	0.007	0.60	0.004	1.24	0.007	20	8
NGC 3384	−3	6	0.56	0.005	1.14	0.008	0.56	0.005	1.17	0.008	20	7
NGC 3390	3	3	0.67	0.012	1.31	0.042	0.62	0.012	1.33	0.042	10	8
NGC 3412	−2	5	0.54	0.005	1.12	0.008	0.55	0.005	1.14	0.008	−5	8
NGC 3432	9	3	0.35	0.018	0.69	0.034	0.38	0.018	0.76	0.034	1	2
NGC 3486	5	3	0.43	0.013	0.86	0.020	0.49	0.013	0.95	0.020	6	3
NGC 3489	−1	5	0.48	0.005	1.05	0.007	0.52	0.005	1.10	0.007	1	1
NGC 3521	4	3	0.54	0.009	1.19	0.012	0.60	0.009	1.16	0.012	6	10
NGC 3556	6	3	0.54	0.013	0.99	0.030	0.56	0.013	1.08	0.030	8	3
NGC 3557	−5	5	0.62	0.005	1.33	0.008	0.62	0.005	1.32	0.008	20	9
NGC 3585	−5	5	0.58	0.005	1.26	0.008	0.59	0.005	1.26	0.008	−5	20
NGC 3607	−2	5	–	–	–	–	0.55	0.005	1.21	0.008	3	3
NGC 3608	−5	5	0.54	0.005	1.12	0.009	0.55	0.005	1.17	0.009	−5	0
NGC 3617	−4	4	0.50	0.011	1.13	0.010	0.55	0.011	1.18	0.010	2	−3
NGC 3626	−1	5	0.49	0.005	0.92	0.009	0.51	0.005	1.01	0.009	−4	3
NGC 3630	−2	5	0.59	0.007	1.20	0.012	0.59	0.007	1.30	0.013	20	3
NGC 3640	−5	5	0.52	0.005	1.22	0.008	0.56	0.005	1.22	0.008	1	20
NGC 3706	−3	6	0.62	0.006	1.32	0.007	0.62	0.006	1.32	0.007	20	20
NGC 3718	1	3	0.55	0.020	1.17	0.036	0.62	0.020	1.30	0.036	5	3
NGC 3733	6	3	0.39	0.028	0.76	0.055	0.37	0.028	0.85	0.055	9	3
NGC 3818	−5	5	0.55	0.007	1.16	0.013	0.55	0.007	1.20	0.013	20	−5
NGC 3872	−5	5	0.62	0.007	1.19	0.012	0.60	0.007	1.25	0.012	9	5
NGC 3877	5	4	0.51	0.013	1.16	0.022	0.59	0.013	1.25	0.022	4	3
NGC 3883	3	2	0.54	0.045	1.06	0.095	–	–	–	–	20	20
NGC 3884	0	2	0.56	0.037	1.15	0.095	–	–	–	–	20	20
NGC 3904	−5	5	0.58	0.005	1.24	0.008	0.58	0.005	1.25	0.008	20	8
NGC 3917	6	3	0.59	0.021	1.12	0.042	0.55	0.021	1.11	0.042	10	9
NGC 3923	−5	5	–	–	–	–	0.63	0.005	1.30	0.008	9	9
NGC 3938	5	4	0.40	0.011	0.89	0.018	0.48	0.011	0.98	0.018	4	3
NGC 3953	4	3	0.54	0.011	1.11	0.015	0.59	0.011	1.19	0.015	6	2
NGC 3957	−1	5	0.61	0.008	1.33	0.015	0.61	0.008	1.31	0.015	20	10

© American Astronomical Society • Provided by the NASA Astrophysics Data System

1995AJ....109..543B

TABLE 5. (continued)

Object	RC3 Type	N	$(V-R)_T$	m.e.	$(V-I)_T$	m.e.	$(V-R)_e$	m.e.	$(V-I)_e$	m.e.	T(SCC) $B-V$	T(SCC) $U-B$
1	2	3	4	5	6	7	8	9	10	11	12	13
NGC 3962	−5	5	0.54	0.005	1.14	0.008	0.58	0.005	1.22	0.008	7	2
NGC 3992	4	4	0.52	0.010	1.05	0.016	0.56	0.010	1.14	0.016	7	3
NGC 4013	3	3	0.64	0.017	1.37	0.030	0.65	0.017	1.40	0.030	−4	7
NGC 4024	−3	5	0.54	0.007	1.19	0.013	0.56	0.007	1.19	0.013	−2	20
NGC 4033	−5	5	0.52	0.006	1.12	0.011	0.56	0.006	1.19	0.011	7	5
NGC 4088	4	2	0.48	0.017	0.96	0.030	0.55	0.021	1.06	0.036	3	3
NGC 4096	5	3	0.47	0.015	0.98	0.025	0.53	0.015	1.07	0.025	2	3
NGC 4100	4	3	0.51	0.015	1.08	0.026	0.58	0.015	1.17	0.026	5	3
NGC 4124	−1	6	0.52	0.008	1.02	0.015	0.55	0.008	1.11	0.015	0	4
NGC 4144	6	3	0.39	0.019	0.81	0.036	0.39	0.019	0.79	0.036	20	10
NGC 4157	3	3	0.59	0.019	1.30	0.029	0.67	0.022	1.40	0.036	4	3
NGC 4179	−2	5	0.57	0.005	1.22	0.008	0.57	0.005	1.22	0.008	20	20
NGC 4183	6	3	0.43	0.026	0.91	0.055	0.51	0.026	1.00	0.055	4	3
NGC 4206	4	4	0.42	0.022	0.91	0.047	0.50	0.022	1.00	0.047	4	3
NGC 4217	3	3	0.56	0.017	1.23	0.032	0.65	0.017	1.33	0.032	4	3
NGC 4233	−2	5	0.52	0.007	1.16	0.013	0.59	0.007	1.24	0.013	5	2
NGC 4261	−5	5	0.60	0.005	1.25	0.009	0.60	0.005	1.26	0.009	20	8
NGC 4281	−1	5	0.57	0.005	1.20	0.012	0.59	0.005	1.25	0.012	0	1
NGC 4365	−5	6	0.60	0.005	1.25	0.008	0.60	0.005	1.25	0.008	20	20
NGC 4371	−1	5	0.61	0.005	1.26	0.008	0.59	0.005	1.24	0.008	9	10
NGC 4374	−5	6	0.58	0.005	1.20	0.008	0.60	0.005	1.24	0.008	−3	−2
NGC 4388	3	3	0.50	0.020	1.12	0.039	0.52	0.020	1.10	0.039	8	10
NGC 4395	9	3	–	–	–	–	0.35	0.037	0.78	0.095	4	3
NGC 4406	−5	6	–	–	–	–	0.57	0.010	1.20	0.015	20	7
NGC 4441	−1	3	0.50	0.026	1.06	0.055	–	–	–	–	10	10
NGC 4449	10	3	0.36	0.008	0.69	0.010	0.34	0.008	0.67	0.010	9	10
NGC 4472	−5	7	–	–	–	–	0.59	0.007	1.23	0.010	20	10
NGC 4476	−3	5	0.54	0.008	1.04	0.016	0.54	0.008	1.13	0.016	20	3
NGC 4507	3	5	0.56	0.008	1.10	0.015	0.54	0.008	1.13	0.015	9	7
NGC 4536	4	3	0.51	0.018	1.06	0.034	0.55	0.018	1.07	0.034	7	8
NGC 4552	−5	5	0.59	0.004	1.22	0.007	0.59	0.004	1.25	0.007	20	7
NGC 4570	−2	3	0.58	0.011	1.17	0.014	–	–	–	–	9	8
NGC 4573	0	5	0.62	0.012	1.26	0.013	0.60	0.012	1.28	0.013	9	8
NGC 4605	5	3	0.42	0.011	0.86	0.014	0.43	0.011	0.88	0.014	−5	7
NGC 4636	−5	6	0.49	0.007	1.18	0.012	0.54	0.007	1.21	0.012	6	7
NGC 4725	2	3	0.47	0.010	1.08	0.014	0.55	0.010	1.17	0.014	4	4
NGC 4729	−4	4	0.57	0.011	1.28	0.010	0.64	0.011	1.38	0.010	5	3
NGC 4731	6	4	0.43	0.019	0.82	0.039	0.39	0.019	0.80	0.039	10	10
NGC 4845	2	3	0.59	0.015	1.19	0.025	0.62	0.015	1.26	0.025	1	2
NGC 4946	−4	11	0.62	0.006	1.34	0.006	0.63	0.006	1.35	0.006	−5	8
NGC 4955	−5	5	0.65	0.010	1.33	0.009	0.63	0.010	1.33	0.009	9	20
NGC 5023	6	3	0.42	0.026	0.83	0.055	0.47	0.026	0.87	0.055	6	−3
NGC 5054	4	5	0.63	0.012	1.18	0.021	0.61	0.012	1.23	0.021	9	1
NGC 5087	−3	6	0.61	0.006	1.32	0.006	0.64	0.006	1.37	0.006	1	1
NGC 5101	0	7	0.58	0.005	1.22	0.008	0.62	0.005	1.27	0.008	1	6
NGC 5124	−5	6	0.59	0.008	1.30	0.008	0.61	0.008	1.32	0.008	0	8
NGC 5170	5	5	0.60	0.014	1.29	0.026	0.64	0.014	1.37	0.026	7	2
NGC 5194	4	3	–	–	–	–	0.50	0.007	1.03	0.009	4	3
NGC 5204	9	2	0.31	0.026	0.63	0.055	0.39	0.032	0.72	0.067	4	3
NGC 5220	1	4	–	–	–	–	0.64	0.014	1.42	0.017	4	3
NGC 5247	4	3	0.48	0.016	0.90	0.032	0.48	0.016	0.97	0.032	20	5
NGC 5248	4	2	0.50	0.016	1.07	0.026	0.54	0.020	1.11	0.032	7	−4
NGC 5297	5	2	0.46	0.022	1.00	0.042	0.55	0.026	1.09	0.042	4	3
NGC 5364	4	3	0.43	0.018	0.94	0.036	0.51	0.018	1.04	0.036	3	3
NGC 5365	−3	5	0.61	0.006	1.32	0.007	0.62	0.006	1.35	0.007	−4	7
NGC 5377	1	3	0.53	0.015	1.18	0.026	0.58	0.021	1.21	0.032	6	7
NGC 5529	5	3	0.65	0.024	1.31	0.047	0.65	0.024	1.34	0.047	20	7
NGC 5585	7	3	0.33	0.018	0.73	0.034	0.39	0.018	0.78	0.034	2	−1
NGC 5670	−2	5	0.66	0.008	1.31	0.009	0.61	0.008	1.29	0.009	10	10
NGC 5676	4	2	0.49	0.021	0.98	0.042	–	–	–	–	4	3
NGC 5701	0	6	0.55	0.011	1.11	0.019	0.57	0.011	1.17	0.019	−2	1
NGC 5746	3	5	0.57	0.012	1.25	0.017	0.64	0.012	1.34	0.017	5	3
NGC 5757	3	6	0.48	0.011	1.00	0.022	0.54	0.011	1.09	0.018	2	3
NGC 5761	−2	5	0.64	0.010	1.29	0.010	0.64	0.010	1.32	0.010	20	7
NGC 5791	−5	8	0.61	0.006	1.25	0.007	0.61	0.006	1.28	0.007	20	7
NGC 5792	3	4	0.68	0.015	1.34	0.025	0.63	0.015	1.32	0.025	10	10
NGC 5796	−5	4	0.56	0.008	1.41	0.016	0.65	0.008	1.39	0.016	4	10
NGC 5812	−5	4	0.61	0.007	1.33	0.012	0.62	0.007	1.32	0.012	−5	9
NGC 5846	−5	4	–	–	–	–	0.61	0.006	1.28	0.011	−4	−4
NGC 5866	−1	2	0.54	0.013	1.14	0.019	–	–	–	–	20	20
NGC 5879	4	3	0.47	0.016	0.98	0.027	0.54	0.021	1.05	0.034	3	5
NGC 5898	−5	7	0.67	0.006	1.40	0.011	0.65	0.006	1.37	0.011	9	10
NGC 5903	−5	8	0.63	0.006	1.24	0.011	0.63	0.006	1.29	0.011	20	1

© American Astronomical Society • Provided by the NASA Astrophysics Data System

1995AJ....109..543B

TABLE 5. (continued)

Object	RC3 Type	N	$(V-R)_T$	m.e.	$(V-I)_T$	m.e.	$(V-R)_e$	m.e.	$(V-I)_e$	m.e.	T(SCC) $B-V$	T(SCC) $U-B$
1	2	3	4	5	6	7	8	9	10	11	12	13
NGC 5907	5	4	–	–	–	–	0.63	0.017	1.30	0.034	0	7
NGC 5921	4	3	0.43	0.021	0.97	0.042	0.51	0.021	1.05	0.042	4	4
NGC 5965	3	3	0.57	0.020	1.26	0.039	0.64	0.020	1.30	0.039	3	−4
NGC 5985	3	3	0.48	0.016	1.01	0.042	0.53	0.016	1.10	0.042	2	3
NGC 5987	3	4	0.59	0.013	1.21	0.021	0.65	0.014	1.30	0.021	2	3
NGC 6012	2	2	0.53	0.022	1.00	0.042	0.51	0.026	1.09	0.047	9	3
NGC 6015	6	2	0.49	0.021	0.98	0.042	0.45	0.028	0.95	0.055	10	10
NGC 6118	6	3	0.55	0.020	1.16	0.039	0.60	0.020	1.24	0.039	2	2
NGC 6140	6	4	0.35	0.018	0.82	0.036	0.43	0.018	0.91	0.036	4	3
NGC 6384	4	5	0.53	0.013	1.11	0.022	0.57	0.013	1.20	0.022	1	3
NGC 6412	5	2	0.37	0.020	0.80	0.039	0.45	0.026	0.90	0.042	4	3
NGC 6503	6	2	0.52	0.015	1.07	0.023	–	–	–	–	10	10
NGC 6643	5	2	0.55	0.021	1.09	0.039	–	–	–	–	10	10
NGC 6661	0	5	0.67	0.008	1.39	0.016	0.67	0.008	1.40	0.016	20	8
NGC 6673	−4	12	0.65	0.004	1.39	0.016	0.63	0.004	1.40	0.016	9	8
NGC 6684	−2	14	0.55	0.003	1.20	0.005	0.57	0.003	1.21	0.005	−3	8
NGC 6690	7	2	0.55	0.026	1.07	0.047	0.50	0.032	1.05	0.055	10	10
NGC 6702	−5	2	0.56	0.022	1.12	0.042	0.62	0.028	1.22	0.047	6	3
NGC 6703	−3	2	0.57	0.015	1.22	0.024	0.60	0.019	1.31	0.027	0	3
NGC 6721	−4	9	0.65	0.006	1.31	0.013	0.63	0.006	1.31	0.013	9	20
NGC 6739	−2	8	0.59	0.006	1.22	0.008	0.55	0.006	1.26	0.008	10	0
NGC 6758	−4	18	0.61	0.004	1.24	0.005	0.61	0.004	1.28	0.005	20	−3
NGC 6771	−1	8	0.58	0.007	1.22	0.014	0.64	0.007	1.32	0.014	2	3
NGC 6782	1	8	0.50	0.006	1.17	0.011	0.57	0.006	1.21	0.011	5	−5
NGC 6794	2	4	0.68	0.013	1.23	0.015	0.66	0.013	1.32	0.015	9	3
NGC 6835	1	6	0.59	0.011	1.20	0.019	0.59	0.011	1.18	0.019	20	10
NGC 6841	−4	4	0.69	0.011	1.44	0.010	0.69	0.011	1.44	0.010	20	20
NGC 6851	−5	9	0.56	0.005	1.17	0.009	0.57	0.005	1.22	0.009	−5	−5
NGC 6854	−3	9	0.55	0.007	1.22	0.015	0.58	0.007	1.25	0.015	0	7
NGC 6861	−3	13	0.60	0.003	1.30	0.005	0.61	0.003	1.32	0.005	−4	8
NGC 6868	−5	13	0.61	0.003	1.28	0.005	0.61	0.003	1.29	0.005	20	8
NGC 6875	−3	17	0.56	0.004	1.18	0.006	0.59	0.004	1.22	0.006	0	−1
NGC 6876	−5	9	–	–	–	–	0.60	0.006	1.26	0.012	20	8
NGC 6893	−2	16	0.60	0.004	1.30	0.006	0.65	0.004	1.39	0.006	6	3
NGC 6902	3	3	0.51	0.026	1.00	0.055	0.49	0.026	1.10	0.055	9	3
NGC 6909	−4	13	0.44	0.005	0.99	0.008	0.49	0.005	1.09	0.008	6	3
NGC 6920	−2	7	0.66	0.006	1.49	0.009	0.62	0.006	1.49	0.009	10	20
NGC 6924	−3	3	0.62	0.013	1.16	0.014	0.60	0.013	1.24	0.014	9	2
NGC 6942	0	10	–	–	–	–	0.55	0.008	1.22	0.019	−5	10
NGC 6946	6	6	–	–	–	–	0.66	0.010	1.40	0.017	4	3
NGC 6958	−4	13	0.55	0.004	1.18	0.007	0.56	0.004	1.18	0.007	−5	20
NGC 7007	−3	11	0.54	0.005	1.17	0.006	0.57	0.005	1.20	0.006	0	7
NGC 7013	0	2	0.62	0.022	1.38	0.047	–	–	–	–	4	3
NGC 7014	−4	8	0.60	0.007	1.20	0.008	0.60	0.007	1.25	0.008	20	6
NGC 7020	−1	13	0.52	0.006	1.08	0.012	0.55	0.006	1.17	0.012	1	3
NGC 7029	−5	9	0.57	0.005	1.17	0.008	0.55	0.005	1.17	0.008	9	20
NGC 7041	−3	13	0.54	0.004	1.19	0.007	0.57	0.004	1.24	0.007	1	0
NGC 7049	−2	13	0.63	0.003	1.30	0.005	0.63	0.003	1.32	0.005	20	8
NGC 7079	−2	20	0.55	0.003	1.15	0.006	0.55	0.003	1.17	0.006	20	8
NGC 7083	4	2	0.44	0.032	0.86	0.067	–	–	–	–	4	3
NGC 7090	5	3	0.44	0.026	0.96	0.055	0.42	0.026	0.94	0.055	9	10
NGC 7097	−5	14	0.54	0.004	1.24	0.007	0.57	0.004	1.23	0.007	0	9
NGC 7126	5	5	0.60	0.008	1.22	0.022	0.58	0.008	1.19	0.022	9	10
NGC 7135	−3	13	0.57	0.005	1.25	0.011	0.59	0.005	1.27	0.011	−2	8
NGC 7144	−5	13	0.53	0.004	1.14	0.006	0.55	0.004	1.19	0.006	8	−1
NGC 7145	−5	13	0.55	0.004	1.17	0.007	0.55	0.004	1.17	0.007	20	20
NGC 7155	−2	9	0.57	0.006	1.24	0.011	0.58	0.006	1.22	0.011	−5	10
NGC 7166	−3	9	0.57	0.005	1.26	0.009	0.59	0.005	1.24	0.009	−2	10
NGC 7168	−5	9	0.58	0.006	1.20	0.011	0.58	0.006	1.23	0.011	20	7
NGC 7180	−2	4	0.56	0.010	1.15	0.009	0.54	0.010	1.15	0.009	9	20
NGC 7184	5	2	0.45	0.028	1.08	0.067	0.53	0.037	1.18	0.095	4	3
NGC 7185	−3	4	0.48	0.011	1.12	0.012	0.52	0.011	1.15	0.012	7	7
NGC 7192	−4	18	0.56	0.004	1.26	0.005	0.57	0.004	1.24	0.005	−5	10
NGC 7196	−5	14	0.56	0.003	1.18	0.006	0.59	0.003	1.25	0.006	1	2
NGC 7213	1	12	0.58	0.003	1.21	0.005	0.58	0.003	1.21	0.005	20	20
NGC 7225	0	4	–	–	–	–	0.61	0.013	1.28	0.015	20	8
NGC 7233	0	6	0.44	0.010	1.01	0.017	0.50	0.010	0.99	0.017	2	10
NGC 7252	−2	4	0.41	0.009	0.93	0.018	0.49	0.009	1.02	0.018	4	3
NGC 7280	−1	2	0.56	0.021	1.16	0.036	–	–	–	–	1	3
NGC 7290	4	2	0.49	0.032	1.02	0.067	–	–	–	–	10	−4
NGC 7292	10	3	0.34	0.022	0.85	0.047	0.38	0.022	0.82	0.047	1	10
NGC 7302	−3	5	0.57	0.008	1.27	0.015	0.59	0.008	1.25	0.016	8	10

© American Astronomical Society • Provided by the NASA Astrophysics Data System

1995AJ....109..543B

TABLE 5. (continued)

Object	RC3 Type	N	$(V-R)_T$	m.e.	$(V-I)_T$	m.e.	$(V-R)_e$	m.e.	$(V-I)_e$	m.e.	T(SCC) $B-V$	T(SCC) $U-B$
1	2	3	4	5	6	7	8	9	10	11	12	13
NGC 7331	3	2	0.60	0.011	1.25	0.014	0.63	0.014	1.35	0.017	1	3
NGC 7332	−2	2	0.53	0.020	1.13	0.039	–	–	–	–	4	10
NGC 7339	4	3	0.57	0.021	1.33	0.039	–	–	–	–	4	10
NGC 7358	−2	4	0.57	0.010	1.20	0.009	0.57	0.010	1.20	0.009	20	20
NGC 7359	−2	8	0.52	0.006	1.18	0.009	0.47	0.006	1.16	0.009	10	10
NGC 7365	−3	4	0.54	0.011	1.11	0.011	0.54	0.011	1.14	0.011	20	7
NGC 7377	−1	6	0.56	0.008	1.18	0.014	0.57	0.008	1.19	0.014	−5	8
NGC 7385	−5	4	–	–	–	–	0.61	0.012	1.35	0.025	20	10
NGC 7393	5	4	0.45	0.020	1.14	0.024	0.54	0.020	1.18	0.024	4	−4
NGC 7410	1	6	0.53	0.005	1.20	0.009	0.56	0.005	1.21	0.009	0	8
NGC 7412	3	6	0.37	0.011	0.81	0.030	0.44	0.011	0.91	0.030	5	3
NGC 7424	6	2	–	–	–	–	0.46	0.045	0.92	0.095	4	20
NGC 7448	4	2	0.44	0.017	0.88	0.027	–	–	–	–	10	10
NGC 7456	6	2	0.46	0.037	0.81	0.095	–	–	–	–	10	3
NGC 7469	1	3	0.61	0.006	1.19	0.042	0.56	0.006	1.16	0.042	10	10
NGC 7479	5	3	0.51	0.015	1.07	0.039	0.58	0.015	1.16	0.039	5	3
NGC 7495	5	2	0.40	0.045	0.80	0.095	–	–	–	–	20	20
NGC 7497	7	6	0.55	0.018	1.05	0.039	0.53	0.018	1.15	0.039	9	3
NGC 7507	−5	17	0.59	0.003	1.26	0.004	0.59	0.003	1.26	0.004	20	20
NGC 7562	−5	6	0.66	0.008	1.27	0.015	0.64	0.008	1.28	0.016	9	8
NGC 7576	−1	4	0.53	0.010	1.19	0.019	0.54	0.010	1.16	0.020	−5	10
NGC 7585	−1	10	0.58	0.004	1.22	0.008	0.56	0.004	1.21	0.008	9	9
NGC 7591	4	2	0.59	0.032	1.16	0.067	–	–	–	–	4	3
NGC 7600	−3	8	0.52	0.006	1.12	0.011	0.53	0.006	1.10	0.011	−4	10
NGC 7606	3	4	0.57	0.016	1.04	0.032	0.53	0.016	1.14	0.032	10	3
NGC 7619	−5	10	0.60	0.006	1.18	0.012	0.61	0.006	1.27	0.013	−3	3
NGC 7626	−5	6	0.66	0.009	1.35	0.019	0.63	0.009	1.33	0.019	9	10
NGC 7633	0	3	0.54	0.012	1.22	0.010	0.62	0.012	1.28	0.010	3	1
NGC 7640	5	2	0.41	0.026	0.86	0.055	0.44	0.032	0.96	0.067	1	3
NGC 7679	−2	5	0.44	0.009	–	–	–	–	–	–	0	–
NGC 7702	−1	10	0.57	0.006	1.17	0.015	0.58	0.006	1.22	0.015	−5	1
NGC 7736	−2	4	0.54	0.012	1.13	0.013	0.58	0.012	1.23	0.013	7	3
NGC 7741	6	3	0.47	0.018	0.94	0.036	0.43	0.018	0.92	0.036	10	9
NGC 7744	−3	21	0.59	0.003	1.24	0.005	0.59	0.003	1.25	0.005	20	8
NGC 7755	5	5	0.67	0.008	1.29	0.021	0.63	0.008	1.26	0.021	10	10
NGC 7785	−5	4	0.63	0.008	1.35	0.016	0.61	0.008	1.33	0.016	9	10
NGC 7793	7	8	–	–	–	–	0.38	0.028	0.87	0.055	7	7
NGC 7796	−4	19	0.58	0.003	1.24	0.005	0.58	0.003	1.24	0.005	20	20
IC 334	0	4	0.76	0.014	1.53	0.024	0.71	0.015	1.52	0.025	10	9
IC 356	2	3	–	–	–	–	0.87	0.024	1.80	0.042	0	3
IC 381	4	2	0.60	0.024	1.22	0.047	0.55	0.028	1.20	0.055	10	10
IC 450	−1	4	0.65	0.012	1.20	0.055	0.63	0.012	1.17	0.055	9	10
IC 983	4	3	0.48	0.024	1.05	0.047	0.56	0.024	1.15	0.047	4	3
IC 1091	3	6	0.54	0.013	1.15	0.024	0.59	0.013	1.25	0.024	6	3
IC 1386	−3	4	0.58	0.012	1.28	0.013	0.60	0.012	1.26	0.013	−4	10
IC 1445	−3	4	0.61	0.011	1.20	0.011	0.56	0.011	1.17	0.011	10	10
IC 1459	−5	12	0.57	0.003	1.24	0.005	0.59	0.003	1.25	0.005	−4	8
IC 1633	−4	7	–	–	–	–	0.58	0.008	1.25	0.009	10	20
IC 1729	−4	4	0.50	0.010	1.12	0.009	0.56	0.010	1.18	0.009	2	5
IC 1812	−4	3	–	–	–	–	0.63	0.012	1.28	0.011	10	9
IC 1895	0	3	0.54	0.013	1.07	0.014	0.54	0.013	1.17	0.014	20	3
IC 1932	0	3	0.59	0.022	1.14	0.036	0.55	0.022	1.12	0.036	10	10
IC 1954	3	4	0.35	0.008	0.77	0.024	0.42	0.008	0.86	0.024	5	3
IC 2006	−5	16	0.54	0.004	1.15	0.005	0.56	0.004	1.18	0.005	8	7
IC 2035	−2	9	0.45	0.004	1.00	0.007	0.48	0.006	0.98	0.009	0	10
IC 2056	4	12	0.47	0.004	0.92	0.008	0.47	0.004	0.95	0.009	20	7
IC 2233	7	4	0.28	0.028	0.65	0.067	0.36	0.028	0.75	0.067	4	3
IC 2311	−5	5	0.61	0.007	1.32	0.007	0.63	0.007	1.35	0.007	−2	7
IC 2437	−3	5	0.61	0.011	1.32	0.013	0.62	0.011	1.32	0.013	−5	20
IC 2533	−3	4	0.58	0.008	1.19	0.008	0.58	0.008	1.24	0.008	20	−4
IC 2580	5	2	0.46	0.028	0.96	0.055	0.54	0.037	0.94	0.067	4	10
IC 2597	−4	2	–	–	–	–	0.63	0.026	–	–	7	–
IC 2977	0	7	0.56	0.011	1.21	0.013	0.58	0.011	1.26	0.013	−3	1
IC 3010	−1	6	0.54	0.011	1.20	0.013	0.56	0.011	1.22	0.013	0	8
IC 3152	−3	4	0.58	0.009	1.21	0.009	0.59	0.009	1.24	0.009	−5	7
IC 3370	−5	5	0.60	0.007	1.25	0.012	0.62	0.007	1.28	0.012	−2	7
IC 4453	−2	5	0.56	0.008	1.22	0.007	0.58	0.008	1.23	0.007	−5	8
IC 4704	−3	9	0.51	0.005	1.26	0.008	0.55	0.005	1.31	0.008	1	0
IC 4797	−4	13	0.58	0.003	1.23	0.006	0.60	0.003	1.27	0.006	−3	6
IC 4864	1	4	0.73	0.017	1.48	0.024	0.74	0.017	1.54	0.024	−5	5
IC 4889	−5	22	0.58	0.003	1.20	0.004	0.58	0.003	1.22	0.004	20	8
IC 4991	−2	4	–	–	–	–	0.57	0.011	1.30	0.010	2	20
IC 5011	0	6	0.57	0.005	1.22	0.007	0.61	0.005	1.25	0.007	7	7
IC 5017	−2	4	–	–	–	–	0.61	0.017	1.31	0.024	10	9

© American Astronomical Society • Provided by the NASA Astrophysics Data System

1995AJ....109..543B

TABLE 5. (continued)

Object	RC3 Type	N	$(V-R)_T$	m.e.	$(V-I)_T$	m.e.	$(V-R)_e$	m.e.	$(V-I)_e$	m.e.	T(SCC) $B-V$	T(SCC) $U-B$
1	2	3	4	5	6	7	8	9	10	11	12	13
IC 5020	4	5	0.44	0.010	1.00	0.024	0.52	0.010	1.09	0.024	4	3
IC 5052	7	2	0.38	0.037	0.88	0.095	0.38	0.045	0.86	0.095	20	10
IC 5063	−1	4	0.67	0.010	1.23	0.019	0.63	0.010	1.28	0.019	10	1
IC 5065	−2	4	0.54	0.013	1.13	0.016	0.51	0.015	1.11	0.017	9	10
IC 5105	−4	14	0.60	0.005	1.24	0.007	0.60	0.005	1.27	0.007	20	7
IC 5131	−3	3	0.55	0.010	1.13	0.009	0.56	0.010	1.20	0.009	−3	5
IC 5161	0	8	0.56	0.004	1.19	0.008	0.59	0.004	1.26	0.008	1	2
IC 5181	−2	14	0.58	0.003	1.24	0.005	0.58	0.003	1.25	0.005	20	8
IC 5267	0	6	0.56	0.007	1.17	0.013	0.59	0.007	1.24	0.013	0	5
IC 5267B	−2	2	–	–	–	–	0.47	0.024	1.03	0.025	4	3
IC 5269	−2	9	0.50	0.007	1.20	0.014	0.53	0.007	1.17	0.014	7	10
IC 5328	−5	22	0.57	0.003	1.21	0.005	0.57	0.003	1.21	0.005	20	20
IC 5353	−3	5	0.54	0.011	1.21	0.029	0.55	0.011	1.20	0.029	−5	9
UGC 3973	3	4	0.59	0.010	0.98	0.047	0.55	0.010	0.95	0.047	10	10
UGC 5456	−2	7	0.33	0.016	0.68	0.032	0.28	0.018	0.66	0.034	10	10
UGC 10288	5	5	0.72	0.032	1.32	0.067	0.68	0.032	1.30	0.067	10	10
MCG −1−24− 1	3	5	0.58	0.015	1.26	0.027	0.66	0.015	1.36	0.027	4	3
MCG −3− 1− 1	10	4	–	–	–	–	0.38	0.024	0.81	0.055	−5	3
ESO 4− 10	−4	6	0.60	0.010	1.23	0.010	0.63	0.010	1.30	0.010	1	5
ESO 5− 10	−5	4	0.63	0.011	1.35	0.011	0.63	0.011	1.37	0.011	20	8
ESO 13− 12	0	10	0.63	0.009	1.32	0.012	0.65	0.009	1.38	0.012	−1	5
ESO 75− 28	−5	5	0.63	0.008	1.26	0.009	0.59	0.008	1.26	0.009	10	20
ESO 84− 26	−1	4	0.56	0.012	1.20	0.012	0.62	0.012	1.25	0.012	5	1
ESO 118− 34	−2	5	0.40	0.012	0.77	0.013	0.36	0.015	0.75	0.015	10	10
ESO 124− 11	−2	4	0.56	0.017	1.35	0.029	0.62	0.017	1.35	0.029	2	20
ESO 126− 14	−2	4	0.76	0.009	1.52	0.008	0.72	0.009	1.51	0.008	10	9
ESO 148− 17	−5	4	0.56	0.010	1.17	0.010	0.54	0.010	1.15	0.010	9	9
ESO 153− 27	0	4	0.59	0.015	1.21	0.019	0.59	0.015	1.24	0.019	20	7
ESO 156− 18	−2	5	0.63	0.015	1.15	0.024	0.61	0.015	1.22	0.024	9	5
ESO 159− 3	−2	5	0.50	0.011	1.06	0.013	0.51	0.011	1.09	0.013	−5	7
ESO 186− 36	1	3	–	–	–	–	0.61	0.014	1.26	0.016	10	10
ESO 197− 10	−2	4	0.56	0.011	1.25	0.010	0.63	0.011	1.32	0.010	5	2
ESO 208− 21	−3	4	–	–	–	–	0.66	0.009	1.40	0.009	20	8
ESO 221− 26	−5	5	0.61	0.006	1.37	0.007	0.63	0.006	1.37	0.007	8	20
ESO 242− 14	−2	4	0.49	0.013	1.09	0.015	0.57	0.013	1.19	0.015	4	3
ESO 256− 11	−2	4	0.64	0.013	1.33	0.017	0.62	0.013	1.33	0.017	9	20
ESO 263− 48	−2	6	0.65	0.009	1.41	0.008	0.67	0.009	1.46	0.008	0	−3
ESO 269− 58	−3	6	0.53	0.015	1.03	0.022	0.49	0.015	1.00	0.022	10	10
ESO 301− 9	−2	4	0.54	0.015	1.05	0.020	0.50	0.015	1.04	0.020	10	9
ESO 316− 42	0	4	0.63	0.016	1.34	0.022	0.63	0.016	1.33	0.022	20	9
ESO 318− 21	0	5	0.59	0.011	1.26	0.012	0.59	0.011	1.28	0.012	20	8
ESO 345− 10	0	6	0.55	0.010	1.05	0.012	0.53	0.010	1.09	0.012	9	−1
ESO 354− 3	−3	4	0.56	0.014	1.13	0.018	0.57	0.014	1.18	0.018	−5	1
ESO 362− 13	−3	4	0.57	0.018	1.19	0.027	0.62	0.018	1.28	0.027	6	3
ESO 367− 8	−2	5	0.69	0.012	1.42	0.015	0.73	0.012	1.51	0.015	7	3
ESO 376− 7	−3	4	0.57	0.011	1.23	0.011	0.58	0.011	1.26	0.011	−3	7
ESO 385− 17	−5	4	0.64	0.012	1.27	0.013	0.59	0.012	1.27	0.013	10	20
ESO 386− 41	0	7	0.60	0.008	1.24	0.007	0.60	0.008	1.28	0.007	20	−5
ESO 387− 16	−5	4	0.61	0.012	1.28	0.013	0.59	0.012	1.29	0.013	9	8
ESO 417− 11	−1	4	0.62	0.014	1.17	0.017	0.59	0.014	1.20	0.017	9	7
ESO 425− 14	−3	6	0.52	0.008	1.18	0.007	0.60	0.008	1.27	0.007	4	3
ESO 437− 45	−2	4	0.58	0.013	1.19	0.016	0.58	0.013	1.24	0.016	20	0
ESO 462− 15	−5	5	0.58	0.009	1.28	0.008	0.61	0.009	1.29	0.008	0	8
ESO 467− 54	−3	4	0.57	0.014	1.29	0.017	0.58	0.014	1.26	0.017	−4	10
ESO 476− 4	−3	4	0.50	0.012	1.13	0.012	0.56	0.012	1.20	0.012	2	5
ESO 479− 33	−2	4	0.61	0.013	1.22	0.014	0.56	0.014	1.28	0.015	10	5
ESO 484− 7	0	5	0.63	0.021	1.28	0.034	0.72	0.022	1.32	0.039	4	−3
ESO 494− 42	−2	4	0.61	0.014	1.27	0.019	0.59	0.014	1.27	0.019	9	20
ESO 500− 2	0	8	0.52	0.014	1.21	0.022	0.60	0.014	1.27	0.022	4	5
ESO 507− 25	−3	6	0.61	0.007	1.27	0.007	0.61	0.007	1.29	0.007	20	8
ESO 541− 13	−4	4	0.46	0.018	1.10	0.026	0.54	0.018	1.19	0.026	4	3
ESO 542− 6	−3	4	0.56	0.014	1.18	0.018	0.60	0.014	1.23	0.018	7	1
ESO 545− 40	−2	4	0.50	0.012	1.09	0.014	0.54	0.012	1.14	0.014	1	1

*Table 5 is presented in its complete form in the AAS CD-ROM Series, Volume 4, 1995.

© American Astronomical Society • Provided by the NASA Astrophysics Data System

1995AJ....109..543B

TABLE 6. Mean total $V-R$ and $V-I$ color indices by type.

T	$<(V-R)^0_T>$	σ	N	$<(V-I)^0_T>$	σ	N	$(V-R)^0_T$ median	$(V-I)^0_T$ median
−5	0.556	0.034	77	1.176	0.058	77	0.56	1.18
−4	0.540	0.042	22	1.154	0.071	22	0.54	1.16
−3	0.548	0.032	52	1.170	0.058	49	0.55	1.17
−2	0.546	0.037	54	1.145	0.069	55	0.55	1.15
−1	0.546	0.034	31	1.144	0.049	30	0.54	1.15
0	0.531	0.027	24	1.107	0.059	25	0.53	1.11
1	0.496	0.041	23	1.039	0.075	22	0.50	1.05
2	0.479	0.034	9	1.018	0.074	10	0.49	1.01
3	0.460	0.056	35	0.933	0.082	34	0.47	0.96
4	0.442	0.041	33	0.928	0.086	33	0.45	0.94
5	0.406	0.073	32	0.868	0.105	29	0.40	0.87
6	0.393	0.056	20	0.799	0.121	21	0.40	0.77
7,8	0.394	0.108	9	0.830	0.173	9	0.36	0.80
9	0.357	0.050	3	0.717	0.103	3	0.35	0.69
10	0.350	0.036	3	0.727	0.040	3	0.36	0.72

TABLE 7. Mean effective $V-R$ and $V-I$ color indices by type.

T	$<(V-R)^0_e>$	σ	N	$<(V-I)^0_e>$	σ	N	$(V-R)^0_e$ median	$(V-I)^0_e$ median
−5	0.571	0.022	91	1.201	0.038	89	0.57	1.20
−4	0.565	0.026	26	1.193	0.051	24	0.57	1.21
−3	0.563	0.025	55	1.198	0.048	53	0.56	1.21
−2	0.553	0.040	58	1.170	0.084	60	0.56	1.19
−1	0.565	0.029	33	1.185	0.050	30	0.57	1.18
0	0.555	0.023	24	1.152	0.046	24	0.56	1.15
1	0.532	0.032	23	1.094	0.065	23	0.53	1.09
2	0.528	0.030	9	1.078	0.054	9	0.52	1.07
3	0.500	0.037	30	1.009	0.080	30	0.50	1.01
4	0.493	0.036	27	0.994	0.081	27	0.49	0.99
5	0.469	0.057	29	0.910	0.139	31	0.47	0.92
6	0.415	0.057	20	0.855	0.108	20	0.41	0.87
7,8	0.394	0.053	10	0.847	0.102	10	0.39	0.85
9	0.373	0.021	3	0.753	0.031	3	0.38	0.76
10	0.360	0.018	4	0.728	0.046	4	0.37	0.74

6. COLOR–TYPE AND COLOR–COLOR RELATIONS

The information in Table 5 of this paper and in Table 4 of Buta & Crocker (1992) allows us to derive the dependence of the average $V-R$ and $V-I$ total and effective colors on revised Hubble type, T, and also the color–color relations involving these color indices. First, it is essential to correct the colors for reddening due to galactic extinction, inclination, and redshift. For galactic and internal reddening, we have used the procedures outlined in the Introduction to RC3, modified for $V-R$ and $V-I$ colors. Cardelli *et al.* (1989) provide a mean extinction law as a function of inverse wavelength x over the range $0.29\ \mu m^{-1} \leq x \leq 8\ \mu m^{-1}$. We have used inverse wavelengths of $1.56\ \mu m^{-1}$ for the Cousins R filter and $1.27\ \mu m^{-1}$ for the Cousins I filter (Bessell 1979) and Eqs. 1, (3a), and (3b) of Cardelli *et al.* to compute the following relationships:

$$\frac{E(V-R)}{E(B-V)} = \frac{0.0767+0.2541/R_V}{-0.0018+1.0495/R_V}, \quad (7a)$$

$$\frac{E(V-I)}{E(B-V)} = \frac{0.2074+0.5479/R_V}{-0.0018+1.0495/R_V}, \quad (7b)$$

where $R_V = A(V)/E(B-V)$ is the ratio of total to selective extinction. In order to be consistent with the corrected $B-V$ and $U-B$ colors in RC3, we have used Eq. (59) of the Introduction to RC3 to compute R_V.

Redshift corrections were made using information in Coleman *et al.* (1980) and Schneider *et al.* (1983). Because most of the galaxies in Table 5 are nearby and have low radial velocities, these corrections are generally less than 0.01 mag.

The least certain corrections are for inclination.[3] The recipe outlined in the Introduction to RC3 was used to obtain $E_i(B-V)$ based on the Hubble type and isophotal axis ratio of each galaxy. Although this recipe may be revised in the near future (see comments in Buta *et al.* 1994), the colors corrected with RC3 procedures still provide a good indication of the dependences of total and effective $V-R$ and $V-I$ colors on Hubble type. These dependences are compiled in Tables 6 and 7 and illustrated in Figs. 3 and 4, respectively. The mean points shown were computed using the procedure described in Sec. *5.3.2* of Buta *et al.* (1994), that is, with a staggered rejection sequence to eliminate the effects of bright emission lines in some early-type galaxies. Figures 3(c),3(d) and 4(c),4(d) show that both total and effective $V-R$ and $V-I$ colors depend significantly on Hubble type. Over the full range of types from $T=-5$ (ellipticals) to $T=10$ (irregulars), the total and effective $V-R$ colors decrease by 0.21 mag while the total and effective $V-I$ colors decrease by about 0.46 mag on average. For comparison, Figs. 3(a),3(b) and 4(a),4(b) show the dependence of the total and effective $B-V$ and $U-B$ colors on type from much larger samples of galaxies (see Buta *et al.* 1994). Over the full range of types, total and effective $B-V$ colors decrease by 0.52 mag while total and effective $U-B$ colors decrease by 0.72 mag on average. These results show that the $V-I$ color index is nearly as sensitive to Hubble type as the $B-V$ color index.

Figures 5(a)–5(d) illustrate the color–color relations involving the $V-R$ and $V-I$ indices. For comparison, Figs. 5(e) and 5(f) show the corresponding $U-B$, $B-V$ correlations for the same samples of galaxies. The $B-V$ and $U-B$ indices are taken from RC3.9a. In each panel, the direction of an average reddening vector is indicated. It is immediately

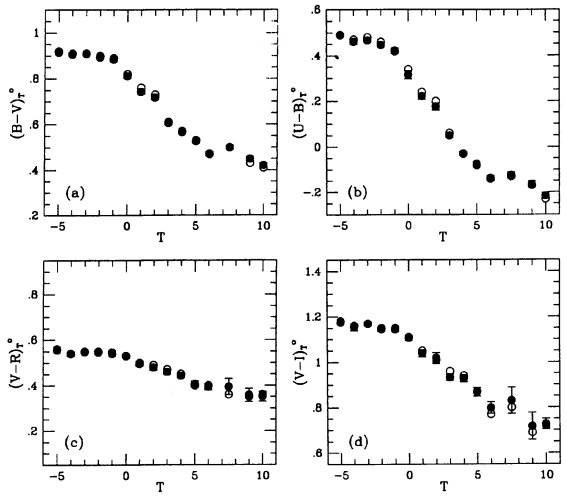

FIG. 3. Mean total $V-R$ and $V-I$ colors vs Hubble type coded on the RC3 numerical scale. Filled circles with error bars are means and open circles are medians. For comparison, the mean total $B-V$ and $U-B$ colors vs type for a larger sample of RC3 galaxies (Buta *et al.* 1994) are also shown.

[3]The issue of the optical depth of spiral galaxy disks is still under considerable debate; see Byun *et al.* (1994) for a recent discussion.

© American Astronomical Society • Provided by the NASA Astrophysics Data System

1995AJ....109..543B

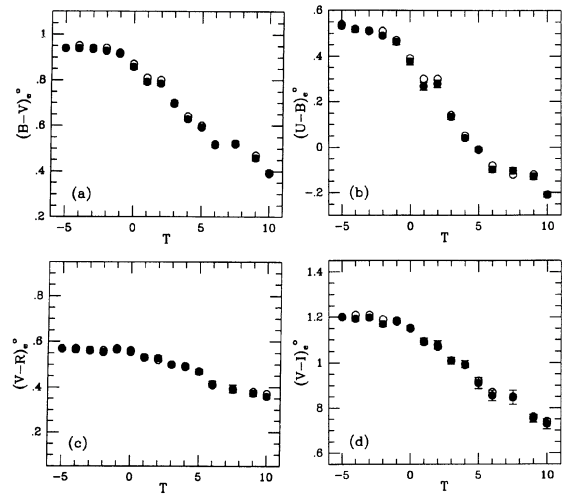

FIG. 4. Mean effective $V-R$ and $V-I$ colors vs Hubble type coded on the RC3 numerical scale. Filled circles with error bars are means and open circles are medians. For comparison, the mean effective $B-V$ and $U-B$ colors vs type for a larger sample of RC3 galaxies (Buta *et al.* 1994) are also shown.

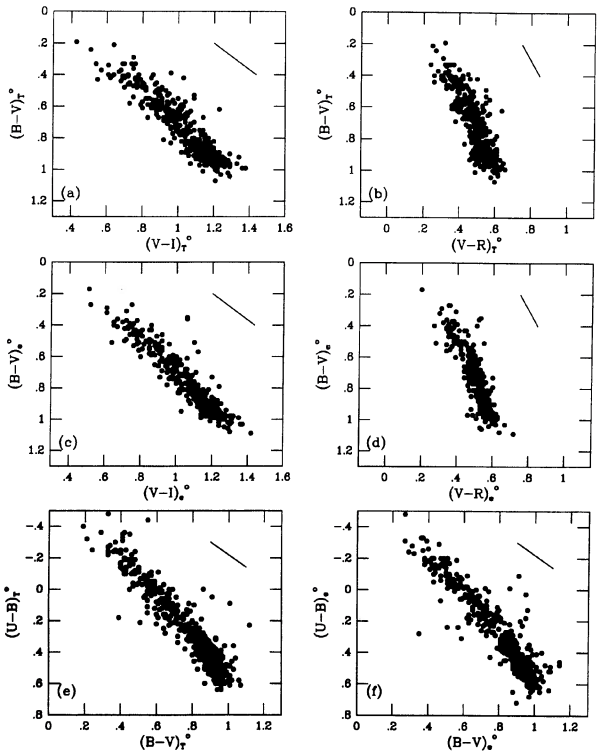

FIG. 5. Two-color plots involving total and effective $V-R$ and $V-I$ colors. The solid line in each case represents the direction of the reddening vector. The plots in (e) and (f) are for the same samples as in (a)–(d). The colors of 32 ringed galaxies from Buta & Crocker (1992) which are not included in Table 5 are also plotted.

clear that uncertainties in the reddening corrections contribute to some of the spreading of the points along the approximately linear correlations, especially for the $B-V$, $V-R$ and $B-V$, $V-I$ correlations. However, the total spread is much larger than the extinction correction uncertainties. The color–color plots shown are similar in the sense that early-type galaxies lie in the lower right sections while late-type galaxies lie in the upper left sections. An extensive interpretation of the $U-B$, $B-V$ diagrams for galaxies is given by Larson & Tinsley (1978).

7. CONCLUSIONS

We have presented in this paper total and effective $V-R$ and $V-I$ color indices for 501 mostly normal bright galaxies over all Hubble types. The color indices were computed using the procedure outlined by Buta *et al.* (1995), and so are homogeneous with the total and effective $U-B$ and $B-V$ color indices presented in RC3. Total and effective $V-R$ and $V-I$ colors have significant dependences on Hubble type. Two-color plots involving these colors are similar to $U-B$, $B-V$ plots but have the disadvantage that the reddening vectors are very nearly parallel to the distribution of points. In any case, the availability now of homogeneously defined total and effective $U-B$, $B-V$, $V-R$, and $V-I$ colors of galaxies should allow greater constraints on models of the star formation history of galaxies. It is anticipated that Table 5 will be supplemented in the future as new *VRI* measurements become available. We note that since our study was carried out, Poulain & Nieto (1994) have published a substantial list of new *UBVRI* photometry of 200 mostly E and S0 galaxies.

We thank H. Corwin for allowing us to utilize his unpublished *VRI* measurements of galaxies, and G. de Vaucouleurs, S. Raychaudhury, and an anonymous referee for helpful comments on the manuscript. This paper was supported by NSF EPSCoR Grant RII 8996152 and NSF REU Grant AST 9300413 to the University of Alabama.

REFERENCES

Aaronson, M. 1978, ApJ, 221, L103
Bessell, M. S. 1979, PASP, 91, 589
Buta, R., & Crocker, D. A. 1992, AJ, 103, 1804
Buta, R., Mitra, S., de Vaucouleurs, G., & Corwin, H. G. 1994, AJ, 107, 118
Buta, R., Corwin, H. G., de Vaucouleurs, G., de Vaucouleurs, A., & Longo, G. 1995, AJ (to be published)
Byun, Y. I., Freeman, K. C., and Kylafis, N. D. 1994, ApJ, 432, 114
Cardelli, J., Clayton, G. C., & Mathis, J. S. 1989, ApJ, 345, 245
Charlot, S., & Bruzual, G. 1991, ApJ, 367, 126
Coleman, G. D., Wu, C.-C., & Weedman, D. W. 1980, ApJS, 43, 393
Corwin, Jr., H. G. 1993, private communication
de Vaucouleurs, G. 1977, ApJS, 33, 211
de Vaucouleurs, G., & Corwin, H. G. 1977, ApJS, 33, 219
de Vaucouleurs, A., & Longo, G. 1988, Catalogue of Visual and Infrared Photometry of Galaxies from 0.5 μm to 10 μm (1961–1985), University of Texas Monographs in Astronomy No. 5

© American Astronomical Society • Provided by the NASA Astrophysics Data System

1995AJ....109..543B

de Vaucouleurs, G., de Vaucouleurs, A., & Corwin, H. 1976, Second Reference Catalogue of Bright Galaxies, University of Texas Monographs in Astronomy No. 2 (RC2)
de Vaucouleurs, G., de Vaucouleurs, A., Corwin, H., Buta, R., Paturel, G., & Forqué, P. 1991, Third Reference Catalogue of Bright Galaxies (Springer, New York) (RC3)
Green, M. R., & Dixon, K. L. 1978, Observatory, 98, 166
Kennicutt, R. C. 1983, ApJ, 272, 54
Larson, R. B., & Tinsley, B. M. 1978, ApJ, 219, 46
Lauberts, A. 1984, A&AS, 58, 249
McAlary, C. W., McLaren, R. A., McGonegal, R. J., & Maza, J. 1983, ApJS, 52, 341
Poulain, P. 1986, A&AS, 64, 236
Poulain, P. 1988, A&AS, 72, 215
Poulain, P., & Nieto, J. L. 1994, A&AS, 103, 573
Schneider, D. P., Gunn, J. E., & Hoessel, J. G. 1983, ApJ, 264, 337
Schroder, M. F. S., & Kepler, S. O. 1991, PASP, 103, 383
Searle, L., Sargent, W. L. W., & Bagnuolo, W. G. 1973, ApJ, 179, 427
Visvanathan, N. 1992, AJ, 103, 1501

© American Astronomical Society • Provided by the NASA Astrophysics Data System